
Los Alamos National Laboratory is operated by the University of California for the United States Department of Energy under contract W-7405-ENG-36

TITLE: THEORETICAL ANALYSES OF (n,xn) REACTIONS ON ^{235}U , ^{238}U , ^{237}Np ,
AND ^{239}Pu FOR ENDF/B-VI

AUTHOR(S): P. G. Young, T-2
E. D. Arthur, T-DO

SUBMITTED TO: The International Conference on Nuclear Data for Science and
Technology, Julich, Germany, May 13-17, 1991

DISCLAIMER

This report was prepared as an account of work sponsored by an agency of the United States Government. Neither the United States Government nor any agency thereof, nor any of their employees, makes any warranty, express or implied, or assumes any legal liability or responsibility for the accuracy, completeness, or usefulness of any information, apparatus, product, or process disclosed, or represents that its use would not infringe privately owned rights. Reference herein to any specific commercial product, process, or service by trade name, trademark, manufacturer, or otherwise does not necessarily constitute or imply its endorsement, recommendation, or favoring by the United States Government or any agency thereof. The view and opinions of authors expressed herein do not necessarily state or reflect those of the United States Government or any agency thereof.

MASTER

By acceptance of this article, the publisher recognizes that the U.S. Government retains a nonexclusive, royalty-free license to publish or reproduce the published form of this contribution, or to allow others to do so, for U.S. Government purposes.

The Los Alamos National Laboratory requests that the publisher identify this article as work performed under the auspices of the U.S. Department of Energy.

Los Alamos Los Alamos National Laboratory
Los Alamos, New Mexico 87545

THEORETICAL ANALYSES OF (n,xn) REACTIONS ON ^{235}U , ^{238}U , ^{237}Np , AND ^{239}Pu FOR ENDF/B-VI

P. G. Young and E. D. Arthur

Theoretical Division, MS B243
Los Alamos National Laboratory
Los Alamos, New Mexico 87545, USA

Abstract: Theoretical analyses were performed of neutron-induced reactions on ^{235}U , ^{238}U , ^{237}Np , and ^{239}Pu between 0.01 and 20 MeV in order to calculate neutron emission cross sections and spectra for ENDF/B-VI evaluations. Coupled-channel optical model potentials were obtained for each target nucleus by fitting total, elastic, and inelastic scattering cross section data, as well as low-energy average resonance data. The resulting deformed optical model potentials were used to calculate direct (n,n') cross sections and transmission coefficients for use in Hauser-Feshbach statistical theory analyses. A fission model with multiple barrier representation, width fluctuation corrections, and preequilibrium corrections were included in the analyses. Direct cross sections for higher-lying vibrational states were calculated using DWBA theory, normalized using $B(E\ell)$ values determined from (d,d') and Coulomb excitation data, where available, and from systematics otherwise. Initial fission barrier parameters and transition state density enhancements appropriate to the compound systems involved were obtained from previous analyses, especially fits to charged-particle fission probability data. The parameters for the fission model were adjusted for each target system to obtain optimum agreement with direct (n,f) cross section measurements, taking account of the various multichance fission channels, that is, the different compound systems involved. The results from these analyses were used to calculate most of the neutron (n,n), (n,n'), and (n,xn) cross section data in the ENDF/B-VI evaluations for the above nuclei, and all of the energy-angle correlated spectra. The deformed optical model and fission model parameterizations are described. Comparisons are given between the results of these analyses and the previous ENDF/B-V evaluations as well as with the available experimental data.

(Keywords: ^{235}U , ^{238}U , ^{237}Np , ^{239}Pu , neutron reactions, data evaluation, nuclear models, coupled-channel optical model, fission theory)

Introduction

We have completed theoretical analyses of neutron-induced reactions on ^{235}U , ^{238}U , ^{237}Np , and ^{239}Pu over the incident energy range 0.01-20 MeV in support of the ENDF/B-VI evaluation effort. Preliminary results from the ^{235}U analysis were reported at the Mito Conference. [1]

The primary purpose for performing the analyses is to provide data on the reactions and energy ranges where little or no experimental data exist, especially for neutron emission reactions and with particular emphasis on odd-A actinides. For most of these nuclei, neutron total and fission cross section measurements exist, [2] so that parameters in the calculations can be optimized to those data. Additionally, limited elastic and inelastic angular distribution data were available for the analyses of ^{235}U , ^{238}U and ^{239}Pu . [3] In the case of $n+^{237}\text{Np}$, however, there were virtually no elastic or inelastic scattering data, only fragmentary information on (n, γ) and (n,2n) reactions, and no experimental data on (n,3n) reactions or secondary neutron energy distributions. The reaction that is best described experimentally for ^{237}Np is fission, as new fission ratio measurements have recently been completed at LAMPF/ANR [4] and Argonne. [5] For all these actinides, prompt nuclear measurements have been made over much of the energy range of interest, but almost no data are available on neutron energy and angular distributions at energies above a few MeV. Therefore, depending on the specific nuclide involved, the main function of the theoretical analyses is to provide total, elastic, inelastic, (n,2n), and (n,3n) cross sections, and in all cases, the angular and energy distributions of secondary neutrons.

Theoretical Analysis and Results

To summarize the analyses briefly, coupled-channel deformed optical model calculations were performed with the ECIS code [6] over the incident neutron energy range from approximately 0.001 to 20 MeV. The starting point for our

optical model analyses were usually extensions [7] of the potentials of Lagrange, [3,8] which were then further modified for the present analysis to improve the calculations above 10 MeV. The role of the coupled-channel calculations in the present analysis are to obtain total, elastic, and ground-state rotational-band (n,n') cross sections, and to provide neutron transmission coefficients for Hauser-Feshbach statistical theory calculations.

The Hauser-Feshbach statistical calculations were performed with the COMNUC [9] and GNASH [10] codes. Both codes include a double-humped fission barrier model, using uncoupled oscillators for the barrier representation in GNASH and coupled or uncoupled oscillators in COMNUC. The COMNUC calculations include width-fluctuation corrections, which are needed at lower energies, whereas GNASH provides the preequilibrium corrections that are required at higher energies. Accordingly, COMNUC was used in the calculations below the threshold for second chance fission (approximately 5 MeV), utilizing fairly strongly damped coupled oscillators. The GNASH code was employed at higher energies, using uncoupled oscillators for second and higher chance fission. Fission transition state spectra were calculated from inputted bandhead parameters or were constructed by taking known (or calculated) energy levels and compressing their spacing by a factor of 2. As usual, Gilbert and Cameron [11] phenomenological level density functions were used to represent continuum levels at ground-state deformations, appropriately matched to available experimental level data. Multiplicative factors were applied to the level density functions to account for enhancements in the fission transition-state densities at barriers due to increased asymmetry conditions.

The fission barrier parameters for the ^{238}U , ^{237}Np and ^{239}Pu calculations are given in Table I. The fission cross sections from the calculations for all four actinides are compared with experimental data in Fig. 1. The dashed curves given in Fig. 1 for the ^{235}U and ^{237}Np cases illustrate the contributions from first-, second-, and third-chance fission.

Table 1. Barrier Parameters Used in the Fission Calculations for ^{238}U , ^{237}Np , and ^{239}Pu .

	n + ^{237}Np Compound Systems			
	^{238}Np	^{237}Np	^{236}Np	^{235}Np
E_A (MeV)	5.87	6.20	5.70	6.40
$\hbar\omega_A$ (MeV)	0.31	0.85	0.50	0.85
E_B (MeV)	5.40	5.50	5.40	5.90
$\hbar\omega_B$ (MeV)	0.36	0.55	0.40	0.55
Density Enhancements:				
Barrier A	4.5	4.5	1.0	1.0
Barrier B	4.5	4.5	1.0	1.0

	n + ^{238}U Compound Systems			
	^{239}U	^{238}U	^{237}U	^{236}U
E_A (MeV)	6.25	5.83	6.03	6.10
$\hbar\omega_A$ (MeV)	0.75	0.50	0.50	0.50
E_B (MeV)	6.00	5.33	5.63	5.90
$\hbar\omega_B$ (MeV)	0.50	0.50	0.50	0.50
Density Enhancements:				
Barrier A	15.	3.8	1.8	1.0
Barrier B	2.	2.0	1.8	1.0

	n + ^{239}Pu Compound Systems			
	^{240}Pu	^{239}Pu	^{238}Pu	^{237}Pu
E_A (MeV)	5.78	5.75	5.65	5.65
$\hbar\omega_A$ (MeV)	0.80	0.63	0.90	1.00
E_B (MeV)	5.46	5.10	5.10	5.10
$\hbar\omega_B$ (MeV)	0.60	0.52	0.85	0.55
Density Enhancements:				
Barrier A	16.	1.1	1.0	2.5
Barrier B	2.	1.1	1.0	2.5

Although most of the direct reaction contribution to inelastic scattering is provided by the coupled-channel calculations of the ground state rotational bands (usually the first three members), additional direct contributions come from vibrational states, generally lying at higher excitation energies. Because of the close spacing of levels in ^{235}U , ^{237}Np , and ^{239}Pu , experimental information on (n,n') reactions to such vibrational states is essentially nonexistent. Therefore, to account for such contributions, we performed distorted-wave Born approximation (DWBA) calculations on nearby even-even nuclei ($^{234,238}\text{U}$, $^{238,240}\text{Pu}$), using reduced transition probabilities $B(E2)$ from (d,d') and Coulomb excitation measurements [12] to obtain absolute (n,n') cross sections, and a weak coupling model [13] to apply the results to states in ^{235}U , ^{237}Np , and ^{239}Pu . The strongest transitions observed in the (d,d') measurements involve population of 3^- and 2^+ vibrational states, corresponding to angular momentum transfers of $\ell=3$ and $\ell=2$, respectively. For ^{237}Np , the deformation parameters needed for normalizing the DWUCK calculations were estimated from systematics, that is, the required $B(E2)$ and $B(E3)$ values were estimated from those determined in the analyses for $^{235,238}\text{U}$ and ^{239}Pu , and all the $\ell=2$ and $\ell=3$ vibrational strength was placed into two fictitious states near $E_x = 1$ MeV. In the case of ^{235}U , the sum of (n,n') cross sections calculated from the dominant $\ell=3$ and $\ell=2$ transitions amounted to approximately 10% of the coupled-channel direct reactions at a neutron energy of 3 MeV, 30% at 8 MeV, and 23% at 20 MeV. While these direct contributions are not large, they do lead to a hardening of the inelastic neutron spectrum that should be included in the ENDF/B-VI evaluations. All the DWBA calculations were performed with the DWUCK code.[14]

As stated above, very limited experimental data exist for elastic scattering, inelastic scattering, and (n,xn) cross sections for the odd-A actinides, and some of the data that do exist are discrepant. In Fig. 2 elastic scattering angular distributions from the ^{239}Pu analysis are compared to experimental data and to earlier ENDF/B evaluations at a few incident energies.

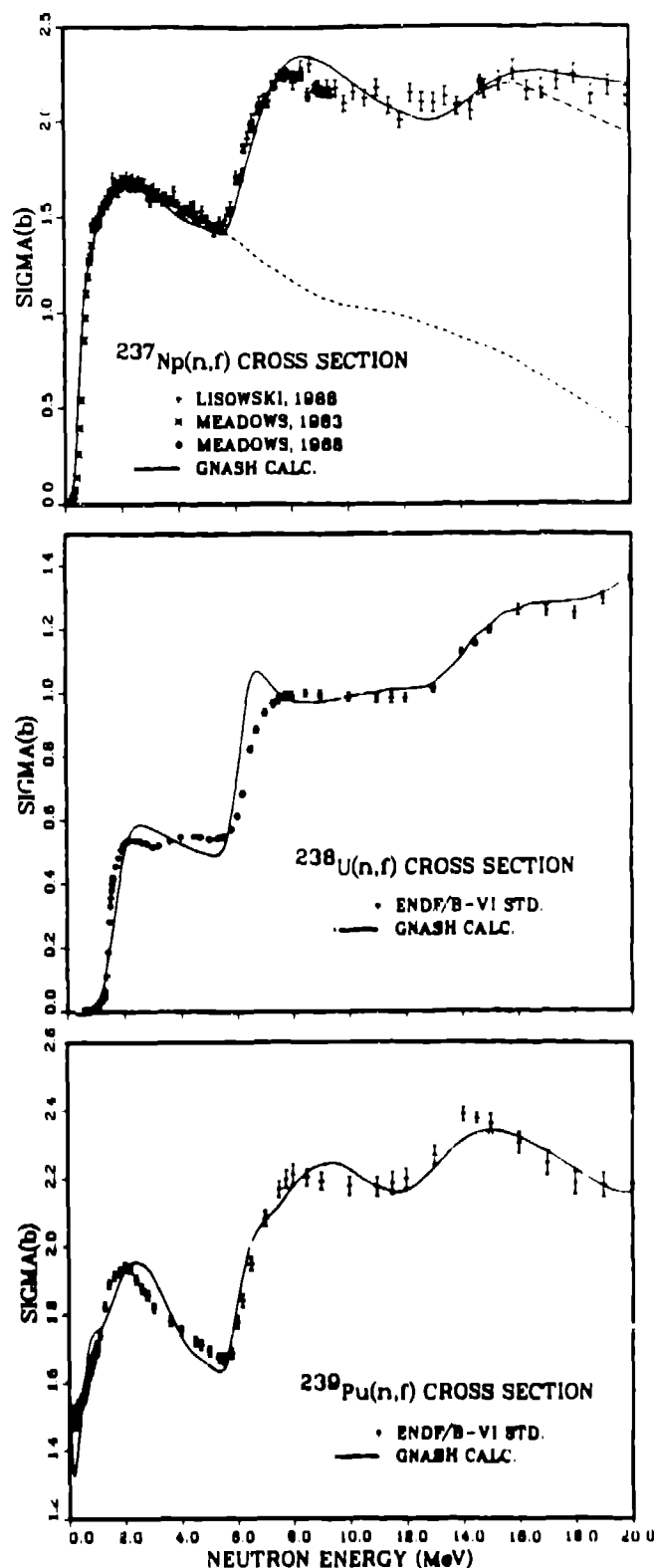


Fig. 1. Calculated and measured neutron-induced fission cross sections for ^{237}Np , ^{238}U , and ^{239}Pu from approximately 50 keV to 20 MeV. The points represent experimental data² and the curves are the results of our theoretical analysis. The dashed and dotted curves shown for ^{237}Np represent the calculated contributions from first-, second-, and third-chance fission.

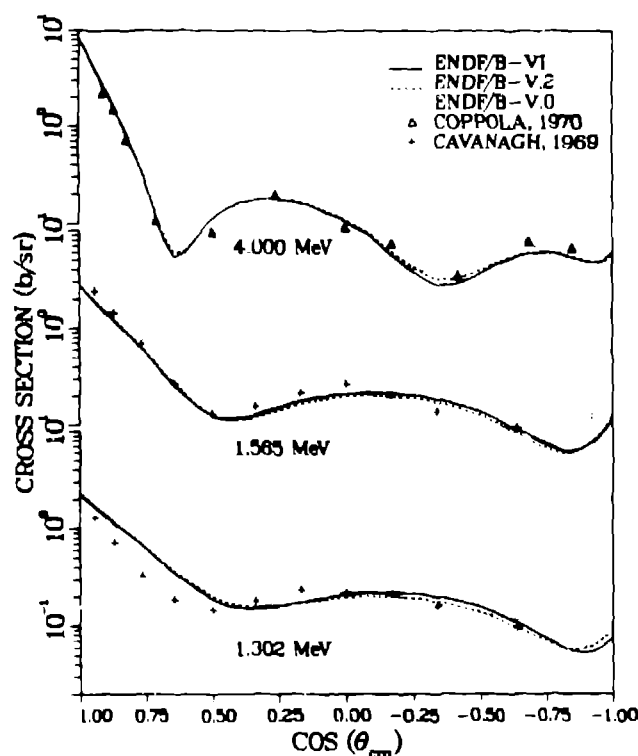


Fig. 2. Experimental and calculated elastic scattering angular distributions for $n + {}^{239}\text{Pu}$ at incident neutron energies of 1.302, 1.565, and 4.0 MeV. The dashed and dotted curves represent previous ENDF/B-V.2 and ENDF/B-V.0 evaluations, respectively.

Comparisons between experimental data and results from the present calculations of the ${}^{239}\text{Pu}(n,n')$ and ${}^{239}\text{Pu}(n,2n)$ cross sections are given in Fig. 3. Also shown

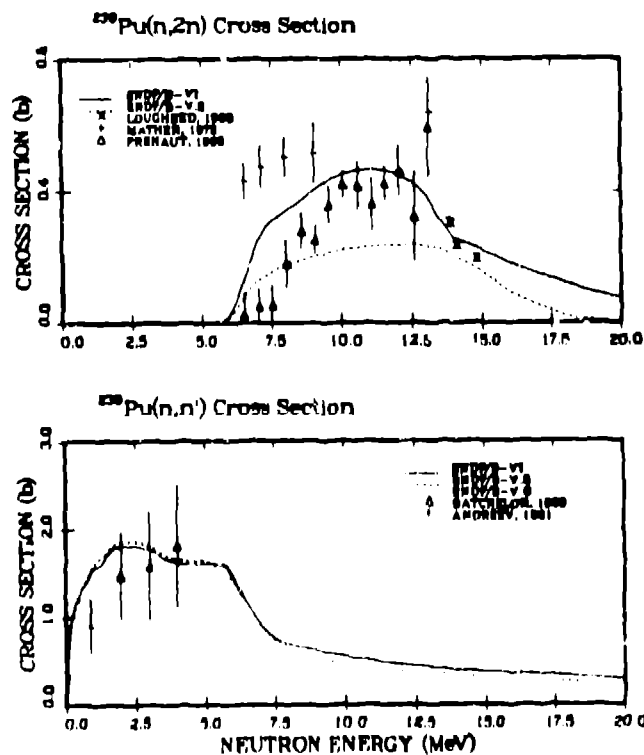


Fig. 3. Calculated and measured $n + {}^{239}\text{Pu}$ inelastic scattering and ${}^{239}\text{Pu}(n,2n){}^{238}\text{Pu}$ cross sections. The dashed and dotted curves represent previous ENDF/B-V.2 and ENDF/B-V.0 evaluations, respectively.

are the previous ENDF/B-V.0 and ENDF/B-V.2 evaluations of these reactions. The present analysis leads to significant improvement in the $(n,2n)$ cross section in the 8-15 MeV region, although discrepancies in the data are apparent. The influence of better accounting for direct reactions results in a somewhat higher (n,n') cross section than the previous ENDF/B-V.0 evaluation, particularly at higher energies.

Conclusions

In conclusion, the present analyses result in substantially improved agreement with the available data for the major odd-A actinides. Except for the fission and total cross sections, which are accurately determined from experiments, results from the present analyses are being used in the MeV region for all major cross sections, angular and energy distributions in the ENDF/B-VI evaluations for ${}^{235}\text{U}$, ${}^{237}\text{Np}$, and ${}^{239}\text{Pu}$. Because more experimental data are available for $n + {}^{238}\text{U}$ reactions, we have used covariance analyses of the experimental data as well as previous ENDF/B-V analyses of data to represent the cross sections for several of the ${}^{238}\text{U}$ reactions, mainly utilizing our theoretical results for continuum neutron energy and angular distributions.

References

1. P. G. Young and E. D. Arthur, in Proc. Int. Conf. on Nuclear Data for Science and Technology, Mito, Japan, May 30 - June 3, 1988 (Ed. S. Igarasi, Saikon Publ. Co., Ltd., 1988), p. 603.
2. Experimental data available from the CSISRS compilation by the National Nuclear Data Center, Brookhaven National Laboratory.
3. G. Haouat, J. Lachkar, Ch. Lagrange, J. Jary, J. Sigaud, and Y. Patin, *Nucl. Sci. Eng.* **81**, 491 (1982).
4. P. W. Lisowski, J. L. Ullmann, S. J. Balestrini, A. D. Carlson, O. A. Wasson, and N. W. Hill, in Proc. Int. Conf. on Nuclear Data for Science and Technology, Mito, Japan, May 30 - June 3, 1988 (Ed. S. Igarasi, Saikon Publ. Co., Ltd., 1988) p. 97.
5. J. W. Meadows, *Nucl. Sci. Eng.* **85**, 271 (1983); J. W. Meadows, *Ann. Nucl. En.* **15**, 421 (1988).
6. J. Raynal, "Optical-Model and Coupled-Channel Calculations in Nuclear Physics," IAEA SMR-9/8, Int. Atomic Energy Agency (1970).
7. P. G. Young, "Rare Earth-Actinide Potentials: ${}^{165}\text{Ho}$, ${}^{238}\text{U}$, ${}^{242}\text{Pu}$," in Applied Nuclear Science Research and Development Semiannual Progress Report (Cps. E. D. Arthur, A. D. Mutschlechner) LA-10689-PR (1986) p. 48.
8. G. Haouat, Ch. Lagrange, J. Lachkar, J. Jary, Y. Patin, and J. Sigaud, in Proc. Int. Conf. on Nuclear Cross Sections for Technology, Knoxville, Tennessee (Oct. 22-26, 1979) p. 672.
9. C. L. Dunford, "A Unified Model for Analysis of Compound Nucleus Reactions," AI-AEC-12931, Atomic International (1970).
10. P. G. Young and E. D. Arthur, "GNASH: A Preequilibrium Statistical Nuclear-Model Code for Calculation of Cross Sections and Emission Spectra," Los Alamos Scientific Laboratory report LA-6947 (Nov. 1977); E. D. Arthur, "The GNASH Preequilibrium-Statistical Model Code," LA UR-88-382 (1988).
11. A. Gilbert and A. G. W. Cameron, *Can. J. Phys.* **43**, 1446 (1965).
12. Y. A. Ellis-Akovali, *Nucl. Data Sheets* **40**, 523 (1983); E. N. Shurshikov, *Nucl. Data Sheets* **38**, 277 (1983).
13. D. M. Brink, *Nucl. Phys.* **4**, 215 (1957); P. Axel, *Phys. Rev.* **126**, 671 (1962).
14. P. D. Kunz, "DWUCK - A Distorted-Wave Born Approximation Program," unpublished.